
Graphical Object-Centric Actor-Critic

Leonid Ugadiarov
FRC CSC RAS
MIPT
ulaelfray@gmail.com

Aleksandr I. Panov
AIRI
FRC CSC RAS
panov@airi.net

Abstract

There have recently been significant advances in the problem of unsupervised object-centric representation learning and its application to downstream tasks. The latest works support the argument that employing disentangled object representations in image-based object-centric reinforcement learning tasks facilitates policy learning. We propose a novel object-centric reinforcement learning algorithm combining actor-critic and model-based approaches to utilize these representations effectively. In our approach, we use a transformer encoder to extract object representations and graph neural networks to approximate the dynamics of an environment. The proposed method fills a research gap in developing efficient object-centric world models for reinforcement learning settings that can be used for environments with discrete or continuous action spaces. Our algorithm performs better in a visually complex 3D robotic environment and a 2D environment with compositional structure than the state-of-the-art model-free actor-critic algorithm built upon transformer architecture and the state-of-the-art monolithic model-based algorithm.

1 Introduction

One of the primary problems in visual-based reinforcement learning is determining how to represent the environment’s state efficiently. The most common approach is to encode the entire input image, which is then used as input for the policy network Mnih et al. [2015], Zhang et al. [2021]. However, previous studies Santoro et al. [2017] have shown that such representations may fail to capture meaningful relationships and interactions between objects in the state. Object-centric representations can be introduced to overcome this issue. Such representations are expected to result in more compact models with enhanced generalization capabilities Keramati et al. [2018]. State-of-the-art unsupervised object-centric representation (OCR) models Singh et al. [2022], Locatello et al. [2020a], Engelcke et al. [2022] have a fundamental appeal for RL as they do not require additional data labeling for training. Recent studies Yoon et al. [2023] have shown that object-centric state factorization can improve model-free algorithms’ generalization ability and sample efficiency.

Another way to reduce the number of necessary environment samples is to use model-based methods Sutton and Barto [2018]. In model-based reinforcement learning (MBRL), the agent constructs models for transition and reward functions based on its experience of interaction with the environment. The agent performs multi-step planning to select the optimal action using the model’s predictions without interacting with the environment. The model-based algorithms could be more efficient than model-free algorithms if the accuracy of the world model is sufficient. State-of-the-art MBRL methods, employing learning in imagination Hafner et al. [2023] and lookahead search with value equivalent dynamics model Ye et al. [2021] master a diverse range of environments.

To further enhance sample efficiency, a promising direction is to combine both approaches by developing a world model that leverages object representations and explicitly learns to model relationships between objects Zholus et al. [2022]. An example of this approach is the contrastively-

trained transition model CSWM Kipf et al. [2020]. It uses a graph neural network to approximate the dynamics of the environment and simultaneously learns to factorize the state and predict changes in the state of individual objects. CSWM has shown superior prediction quality compared to traditional monolithic models.

However, OCR models demonstrate high quality in relatively simple environments with strongly distinguishable objects Wu et al. [2023]. Additionally, in object-structured environments, actions are often applied to a single object or a small number of objects, simplifying the prediction of individual object dynamics. In more complex environments, the world model must accurately bind actions to objects to predict transitions effectively. Despite recent progress Biza et al. [2022], no fully-featured dynamics models considering the sparsity of action-object relationships have been proposed. These challenges make it difficult to employ object-centric world models in RL. For instance, the CSWM model has not been utilized for policy learning in offline or online settings.

Our research is focused on value-based MBRL as object-based decomposition of value function could contribute to the training of object-centric world model consistent with policy. We introduce the Graphical Object-Centric Actor-Critic (GOCA), an off-policy object-centric model-based algorithm inspired by the Soft Actor-Critic (SAC) Haarnoja et al. [2018, 2019], Christodoulou [2019] that operates with both discrete and continuous action spaces. The GOCA algorithm relies on the pre-trained SLATE model Singh et al. [2022], which extracts representations of the individual objects from the input image. Similar to CSWM Kipf et al. [2020], we utilize a structured transition model based on graph neural networks. Our reward, state-value, and actor models are graph neural networks designed to align with the object-centric structure of the task. The GOCA algorithm is the first to apply a GNN-based object-centric world model for policy learning successfully. To evaluate the algorithm’s quality, we conducted experiments in visually complex 3D robotic environments and 2D environments with simple-shaped objects. The proposed algorithm demonstrates high sample efficiency and outperforms the object-oriented variant of the model-free PPO algorithm Schulman et al. [2017], which uses the same SLATE model as a feature extractor and is built upon the transformer architecture. Furthermore, our method performs better than the state-of-the-art MBRL algorithm DreamerV3 Hafner et al. [2023].

2 Related Work

Object-Centric Representation Learning Recent advancements in machine learning research have been dedicated to developing unsupervised OCR algorithms Ramesh et al. [2021], Locatello et al. [2020a], Engelcke et al. [2022]. These methods aim to learn structured visual representations from images without relying on labeled data, modeling each image as a composition of objects. This line of research is motivated by its potential benefits for various downstream tasks, including enhanced generalization and the ability to reason over visual objects. One notable approach in this field is Slot-Attention Locatello et al. [2020a], which represents objects using multiple latent variables and refines them through an attention mechanism. Building upon this, SLATE Ramesh et al. [2021] further improves the performance by employing a Transformer-based decoder instead of a pixel-mixture decoder.

Object-Centric Representations and Model-Free RL ?Heravi et al. [2023] examines RL agents’ performance and generalization capabilities that utilize Slot-Attention as an object-centric features extractor. a multistage training approach is proposed, fine-tuning a YOLO model on a dataset labeled by an unsupervised object-centric model. In another study Sharma et al. [2023], a multistage training approach is proposed, involving fine-tuning a YOLO model Jocher et al. [2022] on a dataset labeled by an unsupervised object-centric model. The frozen YOLO model is then employed as an object-centric features extractor in the Dueling DQN algorithm. Object representations are pooled using a graph attention neural network before being fed to the Q-network.

Object-Centric Representations and MBRL As related work in object-oriented MBRL, we consider Watters et al. [2019]. It uses MONet Burgess et al. [2019] as an object-centric features extractor and learns an object-oriented transition model. However, unlike our approach, this model does not consider the interaction between objects and is only utilized during the exploration phase of the RL algorithm.

3 Background

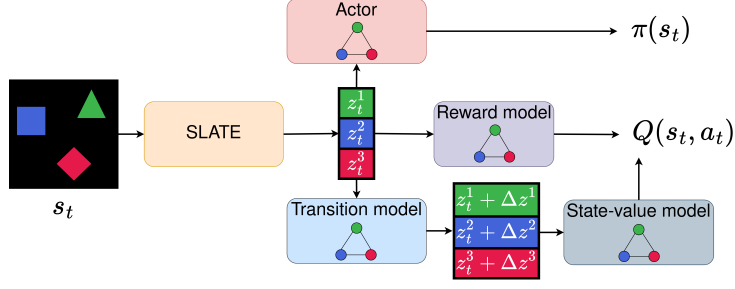


Figure 1: GOCA overview. Framework consists of a pre-trained SLATE model, which extracts object-centric representations from an image-based observation, and GNN-based modules: a transition model, a reward model, a state-value model, and an actor model. The transition and reward models form a world model. The world model and the state-value model together constitute the critic module, which predicts Q-values.

We consider a simplified version of the object-oriented MDP Diuk et al. [2008]:

$$\mathcal{U} = (\mathcal{S}, \mathcal{A}, T, R, \gamma, \mathcal{O}, \Omega), \quad (1)$$

where $\mathcal{S} = \mathcal{S}_1 \times \dots \times \mathcal{S}_K$ — a state space, \mathcal{S}_i — an individual state space of the object i , \mathcal{A} — an action space, $T = (T_1, \dots, T_K)$ — a transition function, $T_i = T_i(T_{i1}(s_i, s_1, a), \dots, T_{iK}(s_i, s_K, a))$ — an individual transition function of the object i , $R = \sum_{i=1}^K R_i$ — a reward function, $R_i = R_i(R_{i1}(s_i, s_1, a), \dots, R_{iK}(s_i, s_K, a))$ — an individual reward function of the object i , $\gamma \in [0; 1]$ — a discount factor, \mathcal{O} — an observation space, $\Omega : \mathcal{S} \rightarrow \mathcal{O}$ — an observation function. The goal of reinforcement learning is to find the optimal policy: $\pi^* = \operatorname{argmax}_{\pi} \mathbb{E}_{s_{t+1} \sim T(\cdot | s_t, a_t), a_{t+1} \sim \pi(\cdot | s_{t+1})} [\sum_{i=0}^{\tau} \gamma^i R(s_t, a_t)]$ for all s_0 where τ is the number of time steps.

Based on the experience of interactions with the environment, the agent can build a world model that approximates the transition function $\hat{T} \approx T$ and the reward function $\hat{R} \approx R$ and use its predictions as an additional signal for policy learning. The accuracy of the world model is crucial for finding the optimal policy: an error-free model allows one to compute the optimal policy without interacting with the environment, but it requires many steps for a deep exploration of the environment and data collection for the world model training. A less accurate model is easier to obtain. Still, erroneous predictions degrade the resulting policy’s quality, especially when using multi-step forecasts when model errors accumulate.

3.1 Soft Actor-Critic

Soft Actor-Critic (SAC) Haarnoja et al. [2018, 2019] is a state-of-the-art off-policy reinforcement learning algorithm for continuous action settings. The goal of the algorithm is to find a policy that maximizes the maximum entropy objective:

$$\pi^* = \operatorname{argmax}_{\pi} \sum_{i=0}^{\tau} \mathbb{E}_{(s_t, a_t) \sim d_{\pi}} [\gamma^i (R(s_t, a_t) + \alpha \mathcal{H}(\pi(\cdot | s_t)))]$$

where α is the temperature parameter, $\mathcal{H}(\pi(\cdot | s_t)) = -\log \pi(\cdot | s_t)$ is the entropy of the policy π at state s_t , d_{π} is the distribution of trajectories induced by policy π . The relationship between the soft state-value function and the soft action-value function is determined as

$$V(s_t) = \mathbb{E}_{a_t \sim \pi(\cdot | s_t)} [Q(s_t, a_t) - \alpha \log(\pi(a_t | s_t))] \quad (2)$$

The soft action-value function $Q_{\theta}(s_t, a_t)$ parameterized using a neural network with parameters θ is trained by minimizing the soft Bellman residual:

$$J_Q(\theta) = \mathbb{E}_{(s_t, a_t) \sim D} [(Q_{\theta}(s_t, a_t) - R(s_t, a_t) - \gamma \mathbb{E}_{s_{t+1} \sim T(s_t, a_t)} V_{\bar{\theta}}(s_{t+1}))^2] \quad (3)$$

where D is a replay buffer of past experience and $V_{\bar{\theta}}(s_{t+1})$ is estimated using a target network for Q and a Monte-carlo estimate of (2) after sampling experiences from the D .

The policy π is restricted to a tractable parameterized family of distributions. A Gaussian policy is often parameterized using a neural network with parameters ϕ that outputs a mean and covariance. The parameters are learned by minimizing the expected KL-divergence between the policy and the exponential of the Q -function:

$$J_{\pi}(\phi) = \mathbb{E}_{s_t \sim D} [\mathbb{E}_{a_t \sim \pi_{\phi}(\cdot|s_t)} [\alpha \log(\pi_{\phi}(a_t|s_t)) - Q_{\theta}(s_t, a_t)]] \quad (4)$$

After reparameterization of the policy with the standard normal distribution, the (4) becomes feasible for backpropagation:

$$J_{\pi}(\phi) = \mathbb{E}_{s_t \sim D, \epsilon_t \sim \mathcal{N}(0,1)} [\alpha \log(\pi_{\phi}(f_{\phi}(\epsilon_t; s_t)|s_t)) - Q_{\theta}(s_t, f_{\phi}(\epsilon_t; s_t))] \quad (5)$$

where action are parameterized as $a_t = f_{\phi}(\epsilon_t; s_t)$.

The objective for the temperature parameter is given by:

$$J(\alpha) = \mathbb{E}_{a_t \sim \pi(\cdot|s_t)} [-\alpha(\log \pi(a_t|s_t) + \bar{H})] \quad (6)$$

where \bar{H} is a hyperparameter representing the target entropy. In practice, two separately trained soft Q-networks are maintained, and then the minimum of their two outputs are used to be the soft Q-network output.

3.2 Soft Actor-Critic for Discrete Action Setting

While SAC solves problems with continuous action space, it cannot be straightforwardly applied to discrete domains since it relies on the reparameterization of Gaussian policies to sample action. A direct discretization of the continuous action output and Q value (SACD) was suggested by Christodoulou [2019]. In the case of discrete action space, $\pi_{\phi}(a_t|s_t)$ outputs a probability for all actions instead of a density. Thus, the expectation (2) can be calculated directly and used in the Q-function objective (3):

$$V(s_t) = \pi(s_t)^T [Q(s_t) - \alpha \log \pi(s_t)] \quad (7)$$

The temperature objective (6) changes to:

$$J(\alpha) = \pi(s_t)^T [-\alpha(\log \pi(s_t) + \bar{H})] \quad (8)$$

The expectation over actions in (4) can be calculated directly, which leads to the policy objective:

$$J_{\pi}(\phi) = \mathbb{E}_{s_t \sim D} [\pi(s_t)^T [\alpha \log(\pi_{\phi}(s_t)) - Q_{\theta}(s_t, \cdot)]] \quad (9)$$

4 Graphical Object-Centric Actor-Critic

Figure 1 outlines the high-level overview of the proposed actor-critic framework (GOCA). A pre-trained object-centric features extractor SLATE takes an image-based observation s_t as input and produces a factored abstract state representation $z_t = (z_t^1, \dots, z_t^K)$ (K - an architectural parameter). An actor model encapsulates the current agent’s policy and returns an action for the input state z_t . Critic predicts the value $Q(z_t, a)$ of the provided action a sampled from the actor given the current state representations z_t . It is estimated using the learned transition model, reward model, and state-value model.

4.1 Observation Model

The SLATE Singh et al. [2022] model is used as an object-centric representations extractor from image-based observations s_t . It consists of a slot-attention module Locatello et al. [2020b], dVAE, and GPT-like transformer Ramesh et al. [2021].

The purpose of dVAE is to reduce an input image of size $H \times W$ into lower dimension representation by a factor of K . First, the observation s_t is fed into the encoder network f_{ϕ} , resulting in log probabilities o_t for a categorical distribution with C classes. Then, these log probabilities are used to sample relaxed one-hot vectors j_t^{soft} from the relaxed categorical distribution with temperature

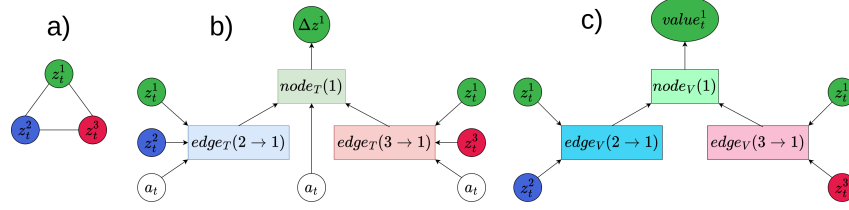


Figure 2: Overview of GNN-based transition model and state-value model. **a)** Representation of the state as a complete graph. **b)** Transition model: message-passing update scheme for the embedding of object 1. **c)** State-value model: message-passing update scheme for the state-value prediction for the object 1.

τ . Each token from j_t^{soft} represents information about $K \times K$ size patch of overall $P = HW/K^2$ patches on the image. After that, j_t^{soft} the vector is being used to reconstruct observation \tilde{s}_t by these patches with the decoder network g_θ .

$$\begin{cases} o_t = f_\phi(s_t) \\ j_t^{\text{soft}} \sim \text{RelaxedCategorical}(o_t; \tau); \\ \tilde{s}_t = g_\theta(j_t^{\text{soft}}). \end{cases}$$

The training objective of dVAE is to minimize MSE between observation s_t and reconstruction \tilde{s}_t :

$$L_{dVAE} = \text{MSE}(\mathbf{s}_t, \tilde{\mathbf{s}}_t), \quad (10)$$

Discrete tokens j_t , obtained from categorical distribution, are mapped to embedding from learnable dictionaries. Those embeddings are summed with learned position embedding p_ϕ to fuse information about patches on the image. Then, the resulting embeddings $u_t^{1:P}$ are fed into the slot attention module. The slot attention returns N object slots $z_t^{1:N}$ and N attention maps $A_t^{1:N}$.

$$\begin{cases} o_t = f_\phi(s_t); \\ j_t \sim \text{Categorical}(o_t); \\ u_t^{1:P} = \text{Dictionary}_\phi(j_t) + p_\phi; \\ z_t^{1:N}, A_t^{1:N} = \text{SlotAttention}_\phi(u_t^{1:P}). \end{cases}$$

The transformer predicts log-probabilities autoregressively \hat{o}_t^i for path i from vectors $\hat{u}_t^{<i}$ generated for previous patches, combined with object centric representations $z_t^{1:N}$. The vector \hat{u}_t^l , $l < i \in [1 : P]$ is formed dictionary embedding from previously generated token \hat{j}_t^l for path l with added position embedding p_ϕ^l . The token \hat{j}_t^i is mapped to the class $c \in C$ with the highest log-probability $\hat{o}_{t,c}^i$. The resulting token can be used to reconstruct observation \hat{s}_t by combining reconstructed patches \hat{s}_t^i .

$$\begin{cases} \hat{u}_t^{<i} = \text{Dictionary}_\phi(\hat{j}_t^{<i}) + p_\phi^i; \\ \hat{o}_t^i = \text{Transformer}_\theta(\hat{u}_t^{<i}; z_t^{1:N}); \\ \hat{j}_t^i = \arg \max_{c \in [1, C]} \hat{o}_{t,c}^i; \\ \hat{s}_t^i = g_\theta(\hat{j}_t^i). \end{cases}$$

The training objective of the transformer is to minimize cross entropy between the distribution of tokens \hat{j}_t generated by the transformer and tokens j_t extracted by dVAE.

$$L_T = \sum_{i=1}^P \text{CrossEntropy}(z_t^i, \hat{z}_t^i) \quad (11)$$

Combining 10 and 11 we receive loss for the SLATE model:

$$L_{SLATE} = L_{dVAE} + L_T$$

4.2 Transition Model

We approximate transition function using a graph neural network Kipf et al. [2020] with an edge model $edge_T$ and a node model $node_T$ which takes a factored state $\mathbf{z}_t = (z_t^1, \dots, z_t^K)$ and action \mathbf{a}_t as input and predicts changes in factored states $\Delta \mathbf{z}$. The action is provided to the node model $node_T$ and the edge model $edge_T$ as shown in Figure 2. The factored representation of the next state is obtained via $\hat{\mathbf{z}}_{t+1} = \mathbf{z}_t + \Delta \mathbf{z}$.

$$\Delta z^i = node_T(z_t^i, a_t^i, \sum_{i \neq j} edge_T(z_t^i, z_t^j, a_t^i)) \quad (12)$$

4.3 Reward Model

The reward model uses almost the same architecture as the transition model. Still, we average object embeddings returned by the node models and feed the result into the MLP to produce the scalar reward. The reward model is trained using the mean squared error loss function with environmental rewards r_t as target (13).

$$\begin{cases} embed_R^i = node_R(z_t^i, a_t^i, \sum_{i \neq j} edge_R(z_t^i, z_t^j, a_t^i)) \\ \hat{R}(\mathbf{z}_t, \mathbf{a}_t) = MLP(\sum_{i=1}^K embed_R^i / K) \end{cases} \quad (13)$$



Figure 3: Examples of observations and slots extracted by the SLATE model in the Object Reaching task (top), Navigation 10x10 task (middle), and Navigation 5x5 task (bottom).

4.4 State-Value Model

The state-value function is approximated using a graph neural network \hat{V} , which does not depend on actions in either the edge model $edge_V$ or the node model $node_V$. As in the reward model, we average object embeddings returned by the node models and feed the result into the MLP to produce the scalar value.

$$\begin{cases} embed_V^i = node_V(z_t^i, \sum_{i \neq j} edge_V(z_t^i, z_t^j)) \\ \hat{V}(\mathbf{z}_t) = MLP(\sum_{i=1}^K embed_V^i / K) \end{cases} \quad (14)$$

4.5 Actor Model

The actor model uses the same GNN architecture as the state-value model but employs different MLP heads for continuous and discrete action spaces. In the case of the continuous action space, it returns the mean and the covariance of the Gaussian distribution. For the discrete action space, it outputs the probabilities for all actions.

$$\begin{cases} embed_{actor}^i = node_{actor}(z_t^i, \sum_{i \neq j} edge_{actor}(z_t^i, z_t^j)) \\ \mu(\mathbf{z}_t) = MLP_{\mu}(\sum_{i=1}^K embed_{actor}^i / K) \\ \sigma^2(\mathbf{z}_t) = MLP_{\sigma^2}(\sum_{i=1}^K embed_{actor}^i / K) \\ \pi(\mathbf{z}_t) = MLP_{\pi}(\sum_{i=1}^K embed_{actor}^i / K) \end{cases} \quad (15)$$

4.6 Critic Output

The action-value function \hat{Q} estimated with the Bellman equation using the transition, reward, and state-value models:

$$\hat{Q}(z_t, a_t) = \hat{R}(z_t, a_t) + \gamma \hat{V}(z_t + \Delta z) \quad (16)$$

4.7 Training

The SLATE model is pre-trained separately on the data set of trajectories collected with a uniform random policy. Following the original paper Singh et al. [2022], we apply decay on the dVAE temperature τ from 1.0 to 0.1 and a learning rate warm-up for the parameters of the slot-attention encoder and the transformer at the start of the training.

To train the models we use SAC objectives (3, 5, 6) for continuous action spaces and SACD objectives (3, 9, 8) for discrete ones. For both scenarios, double Q-network architecture is used. Additionally, we use the data sampled from the replay buffer to train the world model components. The transition model is trained using the mean squared error loss function to minimize the prediction error of the object representations for the next state, given the action. The reward model is trained using the mean squared error loss function with environmental rewards r_t as targets.

$$J_{WM} = \mathbb{E}_{s_t, a_t, r_t, s_{t+1} \sim D} [\beta_T \|z_t + \Delta z - z_{t+1}\|^2 + \beta_R (\hat{R}(z_t, a_t) - r_t)^2] \quad (17)$$

In total, we use four optimizers. The temperature parameter, the actor, and the value model use individual optimizers. The transition and reward models share the world model optimizer.

Due to the stochastic nature of the SLATE model, object-centric representation can shuffle at each step. To enforce the order of object representation during the world model objective (17) optimization, we pre-initialize the slots of the SLATE model for the next state z_{t+1} with the current values z_t .

5 Environments

The efficiency of the proposed GOCA algorithm was evaluated in the 3D robotic simulation environment CausalWorld Ahmed et al. [2020] on the Object Reaching task as it was done in Yoon et al. [2023], and in the compositional 2D environment Shapes2D Kipf et al. [2020] on the Navigation task.

Object Reaching Task In this task, a fixed target object (violet cube) and a set of distractor objects (orange, yellow, and cyan cubes) are randomly placed in the scene. The agent controls a tri-finger robot and must reach the target object with one of its fingers (the other two are permanently fixed) to obtain a positive reward and solve the task. The episode ends without reward if the finger first touches one of the distractor objects. The action space in this environment consists of the three continuous joint positions of the moveable finger. During our experiments, we discovered that one of the baseline algorithms is sensitive to the choice of color scheme for the cubes. Therefore, we also conducted experiments in the task with the original color scheme Yoon et al. [2023]: the color of the target cube is blue, and the colors of the distracting cubes are red, yellow, and green. Examples of observations are shown in the Figure 3.

Navigation Task Shapes2D environment is a four-connected grid world where objects are represented as figures of simple shapes. Examples of observations in the considered versions of the Shapes2D environment are shown in Figure 3. One object — the cross is selected as a stationary target. The other objects are movable. The agent controls all movable objects. In one step, the agent can move an object to any free adjacent cell. The agent aims to collide the controlled objects with the target object. Upon collision, the object disappears, and the agent receives a reward of +1. When an object collides with another movable object or field boundaries, the agent receives a reward of -0.1, and the positions of objects are not changed. For each step in the environment, the agent receives a reward of -0.01. The episode ends if only the target object remains on the field. In the experiments, we use a 5x5-sized environment with five objects and a 10x10-sized environment with eight objects. The action space in the Shapes2D environment is discrete and consists of 16 actions for the Navigation 5x5 task (four movable objects) and 28 actions for the Navigation 10x10 task (seven movable objects).

PushingNoAgent Task The agent controls all movable objects as in the Navigation task, but collisions between two movable objects are permitted: both objects move in the direction of motion. The agent is tasked to push another movable object into the target while controlling the current object. The pushed object disappears, and the agent receives a reward of $+1$ for such an action. When the currently controlled object collides with the target object or field boundaries, the agent receives a reward of -0.1 . When the agent pushes a movable object into the field boundaries, the agent receives a reward of -0.1 . For each step in the environment, the agent receives a reward of -0.01 . The episode ends if only the target object and one movable object remain on the field. In the experiments, we use a 5×5 -sized environment with five objects.

6 Experiments

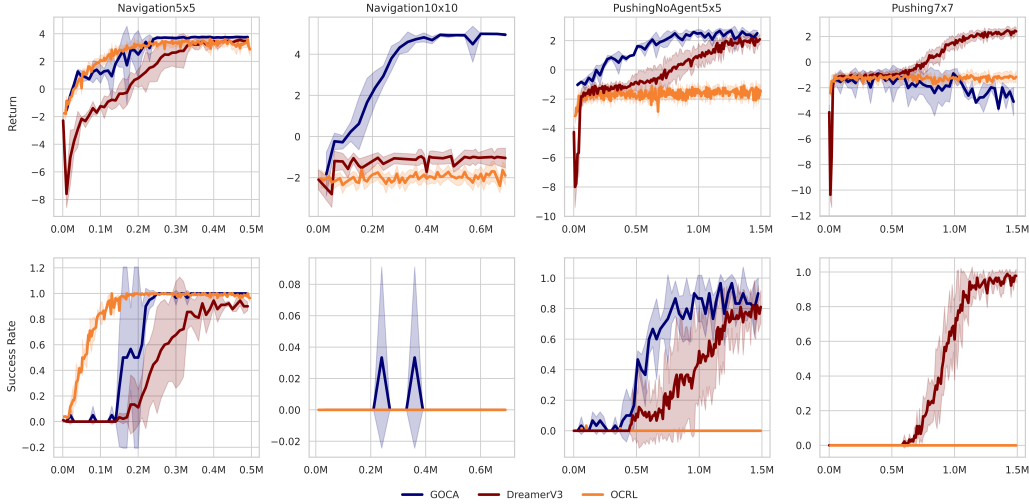


Figure 4: Return and success rate averaged over 30 episodes and three seeds in Shapes2D tasks for GOCA, DreamerV3, and OCRL models. GOCA learns faster or achieves higher metrics than the baselines in all tasks in Shapes2D environment except for Pushing7x7. Shaded areas indicate standard deviation.

We utilize a single SLATE model for Navigation5x5 and PushingNoAgent5x5 tasks as they share the same observation space. However, we train a distinct SLATE model for Navigation10x10 and each version of the Object Reaching task. Appendix A provides detailed information regarding the hyperparameters of the SLATE model.

In continuous Object Reaching tasks, we conventionally use the dimension of the action space as the target entropy hyperparameter for SAC. For 2D tasks with a discrete action space, we scale the entropy of a uniform random policy with the fitted coefficient. For more information on the architecture and hyperparameters of the GOCA model, please refer to Appendix A.

We compare GOCA with a model-free PPO algorithm, using the pre-trained SLATE model as a feature extractor. To combine the latent object representations into a single vector suitable for the value and policy networks of the PPO, we used a Transformer encoder Vaswani et al. [2023] as a pooling layer. We referred to the transformer-based PPO implementation provided by Yoon et al. [2023] as the OCRL baseline. For the Object Reaching Task, we employed the same hyperparameter values as the authors. In contrast, for the Navigation and PushingNoAgent tasks, we utilized the hyperparameter values that the authors used for two-dimensional problems. We used the DreamerV3 Hafner et al. [2023] algorithm as a model-based baseline, with default hyperparameter values from the official repository for all tasks.

Results The graphs in Figures 4 and 5 depict how the episode return of GOCA and the baselines depend on the number of steps for Navigation 5x5, PushingNoAgent5x5, and two versions of the Object Reaching task. For the Navigation 5x5 task, GOCA performs better than the OCRL baseline.

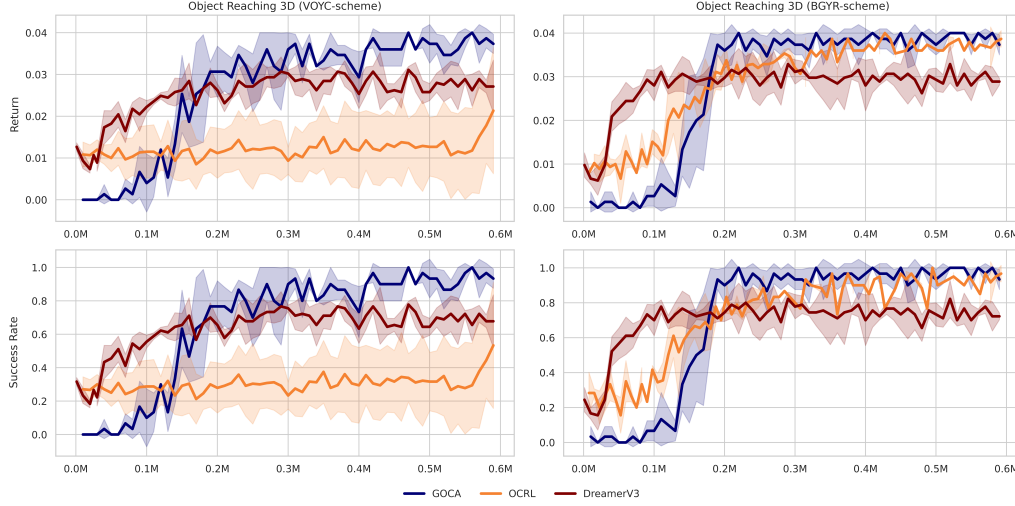


Figure 5: Return and success rate averaged over 30 episodes and three seeds in the Object Reaching task with two color schemes for GOCA, DreamerV3, and OCRL models. GOCA learns faster or achieves higher metrics than the baselines. OCRL baseline is sensitive to the choice of colors used in the environment. Shaded areas indicate standard deviation.

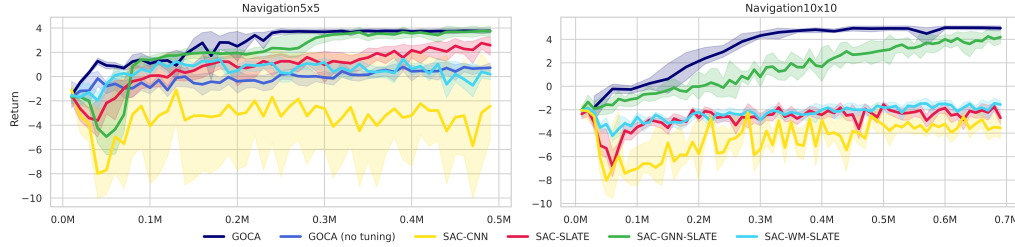


Figure 6: Ablation study. SAC-CNN — a version of SAC with a standard CNN encoder. SAC-SLATE — a version of SAC with a pretrained SLATE encoder which averages object embeddings to obtain the embedding of the current state. SAC-WM-SLATE — a modification of SAC-SLATE which uses a monolithic world-model in its critic. SAC-GNN-SLATE — an object-centric model-free version of SAC with a pretrained SLATE encoder which uses GNNs as actor and critic. GOCA (no-tuning) — a version of GOCA without target entropy tuning. GOCA outperforms the considered baselines. Shaded areas indicate standard deviation.

Although DreamerV3 shows slightly more stable and efficient learning than GOCA, GOCA eventually achieves a higher return. In the PushingNoAgent 5x5 task, GOCA outperforms both baselines. The baselines are initially more effective in the Object Reaching task with our color scheme, but GOCA outperforms them after 200K steps. For the Object Reaching task with the original color scheme, the OCRL baseline demonstrates much better performance, but GOCA also surpasses both baselines after 200K steps. In the more challenging Navigation 10x10 task the both baselines fail to achieve a positive return. GOCA performs better than both baselines but can not solve the task entirely, as it only moves five out of seven objects to the target.

Ablations Figure 6 illustrates the results of additional experiments to estimate the effect of the pre-trained SLATE encoder and the object-centric world model on GOCA’s performance. We evaluate the quality of several monolithic and object-centered versions of SAC. SAC-CNN utilizes the convolutional encoder from the original DQN implementation Mnih et al. [2015]. SAC-SLATE, employs the pre-trained SLATE encoder, whose output embeddings are averaged along the object axis to obtain the permutation-invariant state representation that feeds into the actor and critic MLPs. SAC-WM-SLATE is built on top of the SAC-SLATE and uses a monolithic world model in critic. SAC-GNN-SLATE is an object-centric model-free version of SAC which uses GNN-based actor and

critic. Additionally, we compared GOCA with a variant where the target entropy is set to the default value, equal to the scaled entropy of the uniform random policy with coefficient 0.98 Christodoulou [2019]. Figure 2 illustrates the performance of the considered models. GOCA performs better than SAC-CNN, SAC-SLATE, and GOCA without entropy tuning.

7 Conclusion and Future Work

We presented GOCA, an object-centric off-policy value-based model-based reinforcement learning approach that uses a pre-trained SLATE model as an object-centric feature extractor. Our experiments in 3D and 2D tasks demonstrate that GOCA learns effective policies and outperforms object-centric model-free and model-based baselines. The world model is built upon a GNN architecture, showing that graph neural networks can be successfully applied in MBRL settings for policy learning. However, GOCA does have limitations. Firstly, its world model is deterministic and may struggle to predict the dynamics of highly stochastic environments. Additionally, as our model is based on the SAC algorithm, it is sensitive to the target entropy hyperparameter, especially in environments with discrete action spaces Xu et al. [2021], Zhou et al. [2023].

Our plans include experiments in more challenging environments and research on improving the model’s robustness to changes in hyperparameters.

References

- Ossama Ahmed, Frederik Träuble, Anirudh Goyal, Alexander Neitz, Yoshua Bengio, Bernhard Schölkopf, Manuel Wüthrich, and Stefan Bauer. Causalworld: A robotic manipulation benchmark for causal structure and transfer learning, 2020.
- Ondrej Biza, Robert Platt, Jan-Willem van de Meent, Lawson L.S. Wong, and Thomas Kipf. Binding actions to objects in world models. In *ICLR2022 Workshop on the Elements of Reasoning: Objects, Structure and Causality*, 2022. URL <https://openreview.net/forum?id=HImz8BuUclc>.
- Christopher P. Burgess, Loic Matthey, Nicholas Watters, Rishabh Kabra, Irina Higgins, Matt Botvinick, and Alexander Lerchner. Monet: Unsupervised scene decomposition and representation, 2019.
- Petros Christodoulou. Soft actor-critic for discrete action settings, 2019.
- Carlos Diuk, Andre Cohen, and Michael L. Littman. An object-oriented representation for efficient reinforcement learning. In *Proceedings of the 25th International Conference on Machine Learning, ICML ’08*, page 240–247, New York, NY, USA, 2008. Association for Computing Machinery. ISBN 9781605582054. doi: 10.1145/1390156.1390187. URL <https://doi.org/10.1145/1390156.1390187>.
- Martin Engelcke, Oiwi Parker Jones, and Ingmar Posner. Genesis-v2: Inferring unordered object representations without iterative refinement, 2022.
- Tuomas Haarnoja, Aurick Zhou, Pieter Abbeel, and Sergey Levine. Soft actor-critic: Off-policy maximum entropy deep reinforcement learning with a stochastic actor, 2018.
- Tuomas Haarnoja, Aurick Zhou, Kristian Hartikainen, George Tucker, Sehoon Ha, Jie Tan, Vikash Kumar, Henry Zhu, Abhishek Gupta, Pieter Abbeel, and Sergey Levine. Soft actor-critic algorithms and applications, 2019.
- Danijar Hafner, Jurgis Pasukonis, Jimmy Ba, and Timothy Lillicrap. Mastering diverse domains through world models, 2023.
- Negin Heravi, Ayzaan Wahid, Corey Lynch, Pete Florence, Travis Armstrong, Jonathan Tompson, Pierre Sermanet, Jeannette Bohg, and Debidatta Dwibedi. Visuomotor control in multi-object scenes using object-aware representations, 2023.
- Glenn Jocher, Ayush Chaurasia, Alex Stoken, Jirka Borovec, NanoCode012, Yonghye Kwon, Kalen Michael, TaoXie, Jiacong Fang, Imyhyx, , Lorna, (Zeng Yifu), Colin Wong, Abhiram V, Diego Montes, Zhiqiang Wang, Cristi Fati, Jebastin Nadar, Laughing, UnglvKitDe, Victor

- Sonck, Tkianai, YxNONG, Piotr Skalski, Adam Hogan, Dhruv Nair, Max Strobel, and Mri-nal Jain. ultralytics/yolov5: v7.0 - yolov5 sota realtime instance segmentation, 2022. URL <https://zenodo.org/record/3908559>.
- Ramtin Keramati, Jay Whang, Patrick Cho, and Emma Brunskill. Fast exploration with simplified models and approximately optimistic planning in model based reinforcement learning, 2018.
- Thomas Kipf, Elise van der Pol, and Max Welling. Contrastive learning of structured world models. In *International Conference on Learning Representations*, 2020. URL <https://openreview.net/forum?id=H1gax6VtDB>.
- Francesco Locatello, Dirk Weissenborn, Thomas Unterthiner, Aravindh Mahendran, Georg Heigold, Jakob Uszkoreit, Alexey Dosovitskiy, and Thomas Kipf. Object-centric learning with slot attention, 2020a.
- Francesco Locatello, Dirk Weissenborn, Thomas Unterthiner, Aravindh Mahendran, Georg Heigold, Jakob Uszkoreit, Alexey Dosovitskiy, and Thomas Kipf. Object-centric learning with slot attention, 2020b.
- Volodymyr Mnih, Koray Kavukcuoglu, David Silver, Andrei A. Rusu, Joel Veness, Marc G. Bellemare, Alex Graves, Martin Riedmiller, Andreas K. Fidjeland, Georg Ostrovski, Stig Petersen, Charles Beattie, Amir Sadik, Ioannis Antonoglou, Helen King, Dharshan Kumaran, Daan Wierstra, Shane Legg, and Demis Hassabis. Human-level control through deep reinforcement learning. *Nature*, 518(7540):529–533, February 2015. doi: 10.1038/nature14236. URL <https://doi.org/10.1038/nature14236>.
- Aditya Ramesh, Mikhail Pavlov, Gabriel Goh, Scott Gray, Chelsea Voss, Alec Radford, Mark Chen, and Ilya Sutskever. Zero-shot text-to-image generation, 2021.
- Adam Santoro, David Raposo, David G. T. Barrett, Mateusz Malinowski, Razvan Pascanu, Peter Battaglia, and Timothy Lillicrap. A simple neural network module for relational reasoning, 2017.
- John Schulman, Filip Wolski, Prafulla Dhariwal, Alec Radford, and Oleg Klimov. Proximal policy optimization algorithms, 2017. URL <https://arxiv.org/abs/1707.06347>.
- Vishal Sharma, Aniket Gupta, Prayushi Faldu, Rushil Gupta, Mausam ., and Parag Singla. Object-centric learning of neural policies for zero-shot transfer over domains with varying quantities of interest. In *PRL Workshop Series – Bridging the Gap Between AI Planning and Reinforcement Learning*, 2023. URL <https://openreview.net/forum?id=mQtyk75pYZ>.
- Gautam Singh, Fei Deng, and Sungjin Ahn. Illiterate dall-e learns to compose. In *ICLR*, 2022.
- Richard S. Sutton and Andrew G. Barto. *Reinforcement Learning: An Introduction*. A Bradford Book, Cambridge, MA, USA, 2018. ISBN 0262039249.
- Ashish Vaswani, Noam Shazeer, Niki Parmar, Jakob Uszkoreit, Llion Jones, Aidan N. Gomez, Lukasz Kaiser, and Illia Polosukhin. Attention is all you need, 2023.
- Nicholas Watters, Loic Matthey, Matko Bosnjak, Christopher P. Burgess, and Alexander Lerchner. Cobra: Data-efficient model-based rl through unsupervised object discovery and curiosity-driven exploration, 2019.
- Ziyi Wu, Nikita Dvornik, Klaus Greff, Thomas Kipf, and Animesh Garg. Slotformer: Unsupervised visual dynamics simulation with object-centric models. In *The Eleventh International Conference on Learning Representations*, 2023. URL <https://openreview.net/forum?id=TFbwV6IOVLg>.
- Yaosheng Xu, Dailin Hu, Litian Liang, Stephen McAleer, Pieter Abbeel, and Roy Fox. Target entropy annealing for discrete soft actor-critic, 2021.
- Weirui Ye, Shaohuai Liu, Thanard Kurutach, Pieter Abbeel, and Yang Gao. Mastering atari games with limited data, 2021.
- Jaesik Yoon, Yi-Fu Wu, Heechul Bae, and Sungjin Ahn. An investigation into pre-training object-centric representations for reinforcement learning, 2023.

Amy Zhang, Rowan Thomas McAllister, Roberto Calandra, Yarin Gal, and Sergey Levine. Learning invariant representations for reinforcement learning without reconstruction. In *International Conference on Learning Representations*, 2021. URL <https://openreview.net/forum?id=-2FCwDKRREu>.

Artem Zholus, Yaroslav Ivchenkov, and Aleksandr Panov. Factorized World Models for Learning Causal Relationships. In *ICLR Workshop on the Elements of Reasoning: Objects, Structure and Causality*, 2022. URL <https://openreview.net/forum?id=BCGfDB0Icec>.

Haibin Zhou, Zichuan Lin, Junyou Li, Qiang Fu, Wei Yang, and Deheng Ye. Revisiting discrete soft actor-critic, 2023.

A Appendix

This section presents the architectural parameters of the models utilized in our experiments.

A.1 GOCA

The edge and the node model in GNN-based transition model, reward model, value model and actor model are MLP’s which consists of two hidden layers of 512 units each, LayerNorm and ReLU activations.

Target entropy parameter is set to -3 for Object Reaching task. For tasks with discrete action space we use the scale the entropy of a uniform random policy with coefficient 0.6, which means 1.66 for Navigation 5x5 and PushingNoAgent 5x5 tasks and 2 for Navigation 10x10 task.

Learning	Temp. Cooldown	1
	Temp. Cooldown Steps	30000
	LR for DVAE	0.0003
	LR for CNN Encoder	0.0001
	LR for Transformer Decoder	0.0003
	LR Warm Up Steps	30000
	LR Half Time	250000
	Dropout	0.1
	Clip	0.05
	Batch Size	24
	Epochs	150
DVAE	vocabulary size	4096
CNN Encoder	Hidden Size	64
Slot Attention	Iterations	3
	Slot Heads	1
	Slot Dim.	192
	MLP Hidden Dim.	192
	Pos Channels	4
Transformer Decoder	Layers	4
	Heads	4
	Hidden Dim	192

Table 1: Hyperparameters for SLATE

Gamma	0.99
Buffer size	1000000
Batch size	128
τ_{polyak}	0.005
Buffer prefill size	5000
Number of parallel environments	16

Table 2: Hyperparameters for GOCA